Journal of
Proteomics & Bioinformatics

Tandle et al., J Proteomics Bioinform 2013, S6
DOI: 10.4172/jpb.S6-003

Research Article Open Access

Urinary Metabolomic Profiling of Patients with Glioblastoma Multiforme

Anita T Tandle[1], Uma Shankavaram[1], Meredith V. Brown[2], Jennifer Ho[1], Christian Graves[1], Elena Lita[1], Jeff Pfohl[2], Robert Mohney[2], Philip Tofilon[1] and Kevin Camphausen[1*]

[1]Radiation Oncology Branch, National Cancer Institute, National Institutes of Health, Bethesda, Maryland, USA
[2]Metabolon Inc., Durham, North Carolina, USA

Abstract

With advances in mass spectrometry, gas- and liquid chromatography, it is now feasible to analyze a variety of biofluids for metabolomic changes in a variety of diseases. Recent studies have shown that unique alterations in major metabolic pathways may be present. In this study, the urinary metabolic signature of patients diagnosed with Glioblastoma Multiforme (GBM) was characterized. Metabolomic analysis identified 368 compounds, with forty-six having a significant difference between the samples from patients with GBM, compared to samples from healthy controls. Random forest analysis separated samples from patients with GBM and healthy controls with a 77% accuracy. Using matched urine samples from patients with GBM undergoing chemoirradiation, comparing their sample before irradiation (pre-RT) and after irradiation (post-RT), several N-acetylated compounds were identified as providing the greatest level of distinction between the pre- and post-RT samples. An accumulation of TCA cycle intermediates indicating changes in the mitochondrial oxidative processes was also observed. In summary, our findings identified 46 compounds that differentiated healthy controls from patients with GBM. These may be useful as diagnostic biomarker candidates and highlight the metabolites associated with the pathophysiology of GBM.

Keywords: Glioblastoma multiforme; Metabolomic profiling; Radiation; Urine; GC-MS/MS; LC/MS/MS

Introduction

Glioblastoma Multiforme (GBM) is the most common and most aggressive type of primary brain tumor, with a median survival of 14 months. Currently, the diagnosis of GBM requires surgical resection followed by pathological examination, and the standard therapy for patients with GBM includes maximal tumor resection, irradiation and chemotherapy, using oral temozolomide. Despite this treatment, the vast majority of tumors recur within the irradiation field, thus GBM continues to represent an enormous therapeutic challenge. Though our knowledge of the genome (microarray profile, mutational status and epigenetics) has been well studied for patients with GBM, relatively little is known about the downstream consequences. Using metabolomic profiling on patient samples, one can study the molecules that are the most downstream.

Metabolomics, using mass spectrometry (MS) based techniques, including gas chromatography/mass spectrometry (GC/MS), GC-MS/MS, liquid chromatography/mass spectrometry (LC-MS), and LC-MS/MS, offers an analysis of metabolite levels in biological samples [1,2]. Studies using metabolomics in various cancers, including gastric, lung, renal and colorectal have shown that there are common alterations in metabolism in patients with cancer, but have also shown disease specific alterations in metabolism [3-11]. Because of its peak resolution (ability to separate similar metabolites), high sensitivity and consistent reproducibility, GC/MS has been well established and widely utilized in metabolomic studies [12-14].

The present study examined urine samples from patients with GBM compared to those of healthy controls, to determine if there are GBM-specific metabolites. Toward this end, samples were analyzed using both GC/MS and LC-MS/MS platforms, following protein extraction, allowing maximum recovery of small molecules. Additionally, the urine of patients with GBM pre- and post-radiation (RT) therapy was studied in an effort to identify metabolites of radiation exposure, and possibly radio response.

Materials and Methods

Urine collection and processing

Urine was collected prospectively on clinical study NCI04-C-0200, approved by the Institutional Review Board of the National Cancer Institute, NIH, from 2004 to present. The clinical and pathological characteristics of patients are shown in table 1. We also collected urine samples from 38 healthy untreated volunteers as controls. Samples were centrifuged at 3,000 rpm for 10 min at 4°C, to remove any sediment; supernatant was separated, aliquoted and stored at -20°C [15].

Metabolomics data processing and quality control

Each run included several technical replicate samples, created from a homogeneous pool containing a small amount of all study samples (homogenous pool). Instrument variability was determined by calculating the median Relative Standard Deviation (RSD) for the internal standards that were added to each sample, prior to injection into the mass spectrometers. Overall process variability was determined by calculating the median RSD for all endogenous metabolites (i.e. non-instrument standards), present in 100% of the homogenous pool samples, which are technical replicates of pooled samples. Values for instrument and process variability were 5% and 8%, respectively, within the standard acceptance limits.

***Corresponding author:** Kevin Camphausen, Radiation Oncology Branch, National Cancer Institute, National Institutes of Health, 10 Center Drive B2-3561, Bethesda, MD 20892, USA, Tel: 301-496-5457; Fax: 301-480-5439; E-mail: camphauk@mail.nih.gov

Received February 11, 2013; **Accepted** February 23, 2013; **Published** February 26, 2013

Citation: Tandle AT, Shankavaram U, Brown MV, Ho J, Graves C, et al. (2013) Urinary Metabolomic Profiling of Patients with Glioblastoma Multiforme. J Proteomics Bioinform S6: 003. doi:10.4172/jpb.S6-003

Metabolomic profiling

Global metabolomic profiling was carried out on three independent instrument platforms, to obtain broad coverage of the biochemical classes. This includes one gas chromatography/mass spectrometry (GC/MS), and two ultrahigh performance liquid chromatography/tandem mass spectrometry (LC-MS/MS) platforms optimized for polar compounds, as well as for basic and acidic species. Detailed descriptions of these platforms, including instrumentation configurations and conditions, data acquisition, and software approaches for data handling, were previously described in detail [16,17]. The major components of the process are summarized as follows: Osmolality of the tested urine samples was measured on a Fiske® Model 210 Micro-Sample Osmometer (Fiske Associates, Norwood, MA), using 20 µl of undiluted sample. Undiluted urine samples (100 µl) were extracted using an automated MicroLab STAR® system (Hamilton Company, Salt Lake City, UT), in 450 µl of methanol containing recovery standards.

Table 1: Clinical and pathological characteristics of GBM patients.

Parameter	Samples (n=39)
Sex, no. (%)	
Male	29 (74.4)
Female	10 (25.6)
Age (year)	
Median	55
Range	36-74
Mean	56.1
Std. Dev.	8.7
Age, no. (%)	
<50	5 (12.8)
>50	34 (87.2)
KPS, no. (%)	
≤80	7 (17.9)
>80	32 (82.1)
Median	90
RPA classification, no. (%)	
V	8 (20.5)
IV	26 (66.7)
III	5 (12.8)
Prior Surgery, no. (%)	
Biopsy	8 (20.5)
Subtotal resection	17 (43.6)
Total resection	14 (35.9)
Days from diagnosis to RT (days)	
Median	33
Range	16-54
Mean	34.6
Working/not working	
Working/not working	35 (89.7)
Not working	4 (10.3)

KPS: Karnofsky Performance Score; RPA: Recursive Partitioning Analysis.

The samples were divided into three equal aliquots for analysis in three independent platforms, as described. The samples destined for GC/MS analysis were dried under vacuum desiccation for a minimum of 24 h, and then derivatized under dried nitrogen, using bistrimethyl-silyl-triflouroacetamide. The GC column was 5% phenyl and the temperature ramp was from 40°-300°C in a 16 minute period. Samples were analyzed on a Thermo-Finnigan Trace DSQ fast scanning single-quadrupole mass spectrometer, using electron impact ionization. UPLC/MS was carried out using a Waters Acquity UHPLC (Waters Corporation, Milford, MA), coupled to an LTQ mass spectrometer (Thermo Fisher Scientific Inc., Waltham, MA), equipped with an electrospray ionization source. Two separate UHPLC/MS injections were performed on each sample: one optimized for positive ions and one for negative ions. Chromatographic separation, followed by full scan mass spectra, was carried out to record retention time, molecular weight (m/z) and MS/MS^2 of all detectable ions presented in the samples.

Metabolites were identified by automated comparison of the ion features in the experimental samples to a reference library of chemical standard entries, that included retention time, molecular weight (m/z), preferred adducts, and in-source fragments, as well as their associated MS/MS^2 spectra. This library allowed the rapid identification of metabolites in the experiment with high confidence.

IPA analysis

Expression values for metabolites differentially expressed in GBM pre-RT samples, compared to controls analyzed by Ingenuity Pathway Analysis (IPA). Metabolites were integrated into protein signaling networks, known to be active in GBM.

Statistical analysis

Missing values for a given metabolite were imputed with the observed minimum detection value, based on the assumption that they were below the limits of instrument detection sensitivity. All comparisons were performed using log2-transformed data and median centered data. All samples were normalized to osmolality. Differential expression analysis was performed by Welch's two sample t-tests (GBM *vs.* healthy comparison), or matched pairs t-tests (pre-RT *vs.* post-RT). Multiple comparisons were accounted for with the False Discovery Rate (FDR) method [18]. Random forest analysis was used for predictive modeling and classification of samples into groups (e.g. GBM or healthy).

Random forests produce a single measure of importance for each predictor variable, and take into account interactions among variables, making them more likely to be given high importance relative to other variables. Random forest analyses were performed on selected metabolites at FDR ($q \leq 0.05$), to classify GBM from healthy controls, and to differentiate Post-RT from Pre-RT samples. The accuracy of the predictive model was estimated using X-fold leave out cross validation. Unsupervised analysis was performed by hierarchical clustering, and survival significance of the metabolites was estimated by Kaplan-Meier analysis. We used 25^{th} (q1) and 75^{th} (q4) quartiles for dichotomizing each metabolite for patient samples, in comparison to controls that gave us the most significant relation with outcome, in estimating log rank statistic. All statistical analyses were generated using Array Studio

software or R-bioconductor package (www.bioconductor.org). Array Studio, Array Viewer and Array Server and all other Omicsoft products or service names are registered trademarks or trademarks of Omicsoft Corporation, Research Tringle Park, NC, USA.

Results

Brain MRI

To show the extent of intra-cerebral disease and to demonstrate the typical volumes irradiated in a patient with GBM, figure 1 shows a patient's brain MRI, including an overlay of a standard radiation treatment plan (Figure 1). On the left is a T1, post-contrast MRI, showing a contrast-enhancing lesion in the left parietal lobe before surgery. The middle image shows the same patient's radiation therapy treatment plan. The light blue line encompasses the contrast-enhancing lesion, and the orange line encompasses the non-contrast-enhancing lesion, as defined by T2 MRI (T2 image not shown). The red line represents the area that received the radiation prescription dose of 60 Gy. The right-most image shows the same patient 1 year after treatment, demonstrating a significant decrease in size and enhancement of the original tumor.

Cohort for global metabolomics

To determine if there were metabolites in the urine of patients with GBM that were differentially expressed compared to normal volunteers, metabolomic profiling was performed on three independent instrument platforms, one GC/MS and two LC-MS/MS. A total of 116 urine samples; 38 from healthy volunteers and 39 matched samples from patients, before and after irradiation were studied. Metabolite levels were calculated by automated comparison of the ion features in the experimental samples, to a reference library of chemical standard entries. Following normalization to osmolality, log transformation and imputation with minimum observed values for each compound, we identified a total of 368 named metabolites across all groups.

Urinary metabolomic profiles distinguish GBM patients from healthy controls

To determine whether the 368 metabolites could identify patients with GBM, a Welch's two-sample *t*-test was used.

This identified 46 metabolites that differed significantly ($q \leq 0.05$), between healthy controls and the samples from patients with GBM, before they received radiation (Table 2, Figure 2a). Within the table are listed the biochemical name of each compound, as well as its curated super- and sub-pathways. Fold change values for pre-RT GBM *vs.* control samples, and corresponding p- and q-values are shown for each metabolite. From the 46 differentially expressed molecules, the majority of metabolites [19] were involved in amino acid metabolism, including the sub-pathways of glycine, serine and threonine metabolism (4 metabolites), glutamate metabolism (3 metabolites) and valine, leucine and isoleucine metabolism (3 metabolites) (Table 2). Other pathways included carbohydrate metabolism, lipid metabolism and nucleotide metabolism. The differences between the pre-RT and control samples are highlighted in the heatmap analysis (Figure 2a). In this unsupervised clustering, metabolite values are plotted on the y-axis, and individual samples are on the x-axis, "group". Dark blue coloring within the cluster represent elevated metabolite levels, and yellow represents decreased metabolite levels.

Additionally, along the right most aspect of the cluster, the super-pathway for each metabolite is color coded. To determine if the group of 46 molecules could classify samples as control or GBM, a Random Forest analysis was performed. The 46 molecules had a 77% predictive accuracy (Figure 2b). Thirty of 38 control samples and 29 of 39 pre-radiation samples were correctly classified. Thus, the metabolites that are differentially expressed between the two groups may represent potential biomarkers for GBM.

Metabolites associated with improved survival

To determine if the metabolite levels in patients with GBM correlated with survival, we used Kaplan-Meier analysis. Of the 46 metabolites, 6.5% showed a difference in patient survival, including mannitol, pyroglutamine and 7-methylguanine, when the values across all the samples were divided into quartiles (Figure 3). Mannitol was elevated in samples from patients with GBM compared to controls (2.2 GBM/control), and Kaplan-Meier analysis showed that GBM patients having low mannitol levels (<qt1) had better survival (12.1 months, P=0.0263), compared to patients with high mannitol levels (>qt4, 5.5 months) (Figure 3a). Pyroglutamine (0.76 GBM/control) and 7-

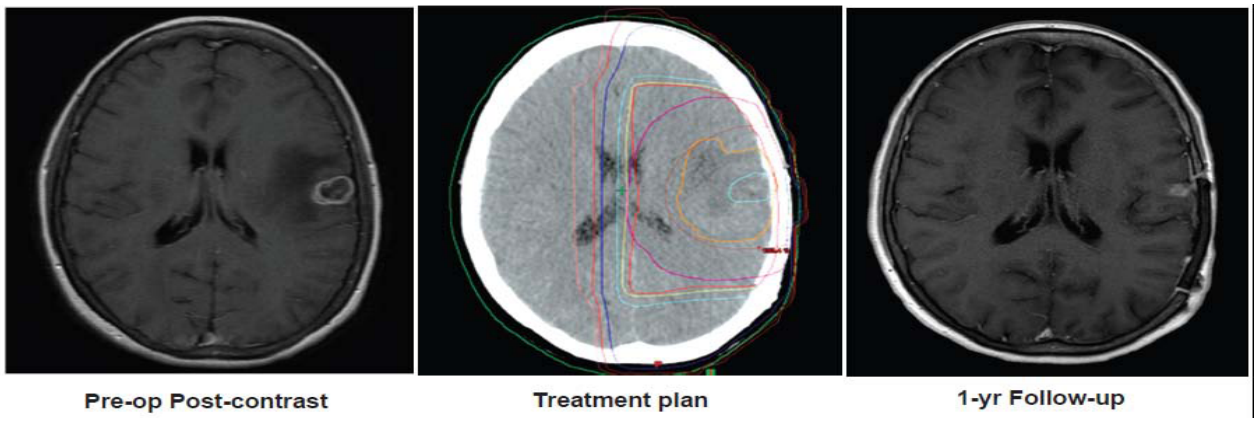

Figure 1: A brain MRI image of one representative patient from this study, depicting a standard treatment plan for GBM. On the left is a T1, post-contrast MRI, showing a contrast-enhancing lesion in the left parietal lobe before surgery and before radiation therapy. The middle image shows the same patient's treatment plan. The light blue line encompasses the contrast-enhancing lesion, and the orange line encompasses the non-contrast-enhancing lesion, as defined by T2 MRI. The red line represents the area that received the prescription dose of 60 Gy total. The right-most image shows the same patient 1 year after treatment.

Table 2: Urinary metabolomic profile distinguishes GBM patients from healthy controls.

BIOCHEMICAL NAME	KEGG	HMDB	SUPER PATHWAY	SUB PATHWAY	Pre-RT GBM/Control			
					Welch's Two-sample t-test			Log-rank t-test
					Fold Change	*p*-Value	*q*-Value	
serine	C00065	HMDB03406	Amino acid	Glycine, serine and threonine metabolism	0.63	<0.001	0.0071	0.0149
glycine	C00037	HMDB00123	Amino acid	Glycine, serine and threonine metabolism	0.64	<0.001	0.0063	0.021
guanidinoacetate	C00581	HMDB00128	Amino acid	Guanidino and acetamido metabolism	0.40	<0.001	0.0033	0.299
4-acetamidobutanoate	C02946	HMDB03681	Amino acid	Guanidino and acetamido metabolism	1.44	<0.001	0.0003	0.681
urea	C00086	HMDB00294	Amino acid	Urea cycle; arginine-, proline-, metabolism	1.35	<0.001	0.0063	0.736
tigloylglycine		HMDB00959	Amino acid	Valine, leucine and isoleucine metabolism	0.67	<0.001	0.0027	0.89
cysteine	C00097	HMDB00574	Amino acid	Cysteine, methionine, SAM, taurine metabolism	1.67	<0.001	0.0071	0.9
N-acetylneuraminate	C00270	HMDB00230	Carbohydrate	Aminosugars metabolism	1.64	<0.001	0.0057	0.962
pyridoxate	C00847	HMDB00017	Cofactors and vitamins	Vitamin B6 metabolism	3.39	<0.001	0.0071	0.21
carnosine	C00386	HMDB00033	Peptide	Dipeptide derivative	0.34	<0.001	0.0014	0.0371
glycolate (hydroxyacetate)	C00160	HMDB00115	Xenobiotics	Chemical	0.72	<0.001	0.0071	0.0412
isobutyrylglycine		HMDB00730	Amino acid	Valine, leucine and isoleucine metabolism	1.62	0.0010	0.0076	0.872
pyroglutamine*			Amino acid	Glutamate metabolism	0.76	0.0017	0.0119	0.351
ethylmalonate		HMDB00622	Lipid	Carnitine metabolism	1.50	0.0017	0.0119	0.0625
nicotinamide	C00153	HMDB01406	Cofactors and vitamins	Nicotinate and nicotinamide metabolism	2.47	0.0018	0.0123	0.807
taurocholenate sulfate*			Lipid	Bile acid metabolism	0.64	0.0019	0.0124	0.928
kynurenine	C00328	HMDB00684	Amino acid	Tryptophan metabolism	1.65	0.0025	0.0154	0.744
glycocholenate sulfate*			Lipid	Bile acid metabolism	0.62	0.0030	0.0181	0.771
N-carbamylglutamate	C05829		Amino acid	Glutamate metabolism	1.70	0.0032	0.0186	0.783
xanthurenate	C02470	HMDB00881	Amino acid	Tryptophan metabolism	0.65	0.0035	0.0198	0.49
imidazole lactate	C05568	HMDB02320	Amino acid	Histidine metabolism	0.48	0.0042	0.0225	0.191
tiglyl carnitine		HMDB02366	Amino acid	Valine, leucine and isoleucine metabolism	0.75	0.0043	0.0225	0.502
guanidine		HMDB01842	Nucleotide	Purine metabolism, guanine containing	1.60	0.0047	0.0238	0.774
4-hydroxyphenylpyruvate	C01179	HMDB00707	Amino acid	Phenylalanine & tyrosine metabolism	0.40	0.0056	0.0267	0.761
dihydrobiopterin	C02953,C00268	HMDB00038	Cofactors and vitamins	Folate metabolism	0.64	0.0056	0.0267	0.965
3-methyl-2-oxovalerate	C00671	HMDB03736	Amino acid	Valine, leucine and isoleucine metabolism	0.59	0.0057	0.0267	0.686
anserine	C01262	HMDB00194	Peptide	Dipeptide derivative	0.12	0.0064	0.0291	0.0375
choline	C00114	HMDB00097	Lipid	Glycerolipid metabolism	1.39	0.0065	0.0291	0.499
2-(4-hydroxyphenyl)propionate	C03080		Amino acid	Phenylalanine & tyrosine metabolism	0.25	0.0068	0.0297	0.794
trigonelline (N'- ethylnicotinate)	C01004	HMDB00875	Cofactors and vitamins	Nicotinate and nicotinamide metabolism	1.59	0.0076	0.0320	0.464

1-methylhistidine	C01152	HMDB00001	Amino acid	Histidine metabolism	0.55	0.0080	0.0325	0.0338
dimethylglycine	C01026	HMDB00092	Amino acid	Glycine, serine and threonine metabolism	0.73	0.0081	0.0325	0.675
allantoin	C02350	HMDB00462	Nucleotide	Purine metabolism, urate metabolism	2.30	0.0086	0.0334	0.196
sucrose	C00089	HMDB00258	Carbohydrate	Fructose, mannose, galactose, starch, and sucrose metabolism	2.29	0.0087	0.0334	0.674
gallate	D01398,C01424	HMDB05807	Xenobiotics	Food component/ Plant	0.51	0.0088	0.0334	0.382
N4-acetylcytidine		HMDB05923	Nucleotide	Pyrimidine metabolism, cytidine containing	1.51	0.0090	0.0334	0.948
riboflavin (Vitamin B2)	C00255	HMDB00244	Cofactors and vitamins	Riboflavin metabolism	3.46	0.0107	0.0389	0.455
N2-acetyllysine	C12989	HMDB00446	Amino acid	Lysine metabolism	1.35	0.0111	0.0394	0.257
7-methylguanine	C02242	HMDB00897	Nucleotide	Purine metabolism, guanine containing	0.83	0.0114	0.0396	0.0223
mannitol	C00392	HMDB00765	Carbohydrate	Fructose, mannose, galactose, starch, and sucrose metabolism	2.20	0.0117	0.0396	0.0803
taurolithocholate 3-sulfate	C03642	HMDB02580	Lipid	Bile acid metabolism	0.47	0.0119	0.0396	0.312
glutamine	C00064	HMDB00641	Amino acid	Glutamate metabolism	1.51	0.0138	0.0453	0.706
homocitrulline	C02427	HMDB00679	Amino acid	Urea cycle; arginine-, proline-, metabolism	1.44	0.0145	0.0453	0.0908
threonate	C01620	HMDB00943	Cofactors and vitamins	Ascorbate and aldarate metabolism	2.62	0.0146	0.0453	0.182
phosphate	C00009	HMDB01429	Energy	Oxidative phosphorylation	1.23	0.0146	0.0453	0.727
threonine	C00188	HMDB00167	Amino acid	Glycine, serine and threonine metabolism	0.74	0.0161	0.0490	0.0115
Red represents increase and green represents decrease fold changes								
KEGG: Kyoto Encyclopedia of Genes and Genomes; HMDB: The Human Metabolome Database								

methylguanine (0.83 GBM/control) levels were both reduced in GBM patients, compared to controls (Figure 3b and 3c). For both metabolites, the patient survival was 4 months in patients that had lower levels (in <qt1) verses 10.1 months in patients that had higher levels (in >qt4), with p=0.029 and p=0.00482, respectively. Whether these metabolites are GBM specific or related to general tumor metabolism will require further detailed study.

IPA analysis

To further define the molecular pathways that may be involved in GBM pathology, we used IPA to analyze the 46 metabolites, differentially expressed between control and GBM urine samples. The top network with a score of 37, had 15 (out of 46) molecules that were differentially expressed between control and GBM urine samples. The top three Molecular and Cellular Functions are associated with amino acid metabolism (8 metabolites), small molecule biochemistry (19 metabolites), and molecular transport (16 metabolites). The top network is shown in figure 4. This network has the metabolites that were over-expressed in the samples from patients with GBM, highlighted in red, and the under expressed metabolites highlighted in green. Furthermore, by expanding the metabolite network to include signaling molecules pre-defined by IPA, we show that these metabolites are interconnected by signaling molecules known to be involved in GBM pathology, including PI3K, AKT, ERK and ERK1 [20,21]. As large scale genomic analysis of GBM has demonstrated that these signaling pathways are often mutated in GBM, these abnormally expressed metabolites may represent the end product of these abnormal signaling pathways [22].

Radiation-induced changes in urine metabolites

Next, we explored if radiation treatment resulted in any changes in the patient's urine metabolite profile. We compared metabolite levels in GBM patient's pre and post-RT using random forest analysis. A predictive accuracy of 73% could be obtained for classifying all GBM samples into either pre- or post-radiation treatment groups (Figure 5a). The confusion matrix in figure 5a shows that 26 out of 39 post-RT samples were correctly classified, whereas 31 of the 39 pre-RT samples were correctly classified. Notably, N-acetylated metabolites, including N-acetylphenylalanine, Nacetyltryptophan, N-acetyltyrosine, and N-acetylproline were significantly elevated in patient urine post-RT. Additionally, TCA cycle intermediates, including citrate, iso-citrate, alpha-ketoglutarate, succinate, fumarate, malate and 2-hydroxyglutarate were significantly elevated post-RT (Figure 5b). Thus, there is potentially a set of metabolites following irradiation that are distinct from those found in patients with GBM, that may be useful as biomarkers of radiation exposure.

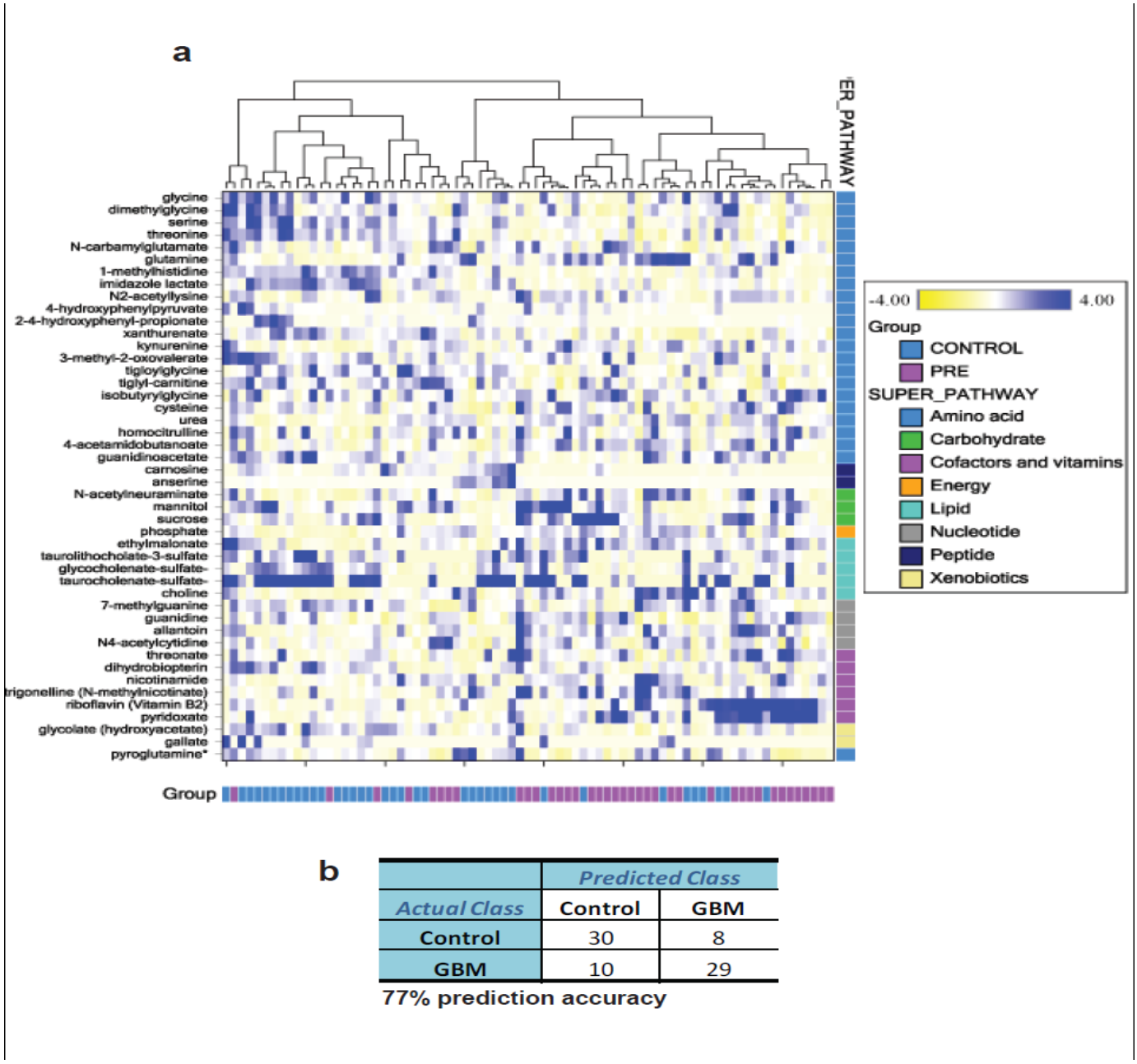

b

	Predicted Class	
Actual Class	Control	GBM
Control	30	8
GBM	10	29

77% prediction accuracy

Figure 2: Urinary metabolomic profile distinguish GBM patients from healthy controls. (a) Welch's two-sample *t*-test was used to identify metabolites that differed significantly between GBM groups (magenta), compared to control (untreated healthy, blue). In this unsupervised clustering, metabolite values are plotted on the y-axis and individual samples are on the x-axis, "group". Dark blue coloring within the cluster, represent elevated metabolite levels and yellow represents decreased metabolite levels. Additionally, along the right most aspect of the cluster the super-pathway for each metabolite is colorcoded.

(b) The confusion matrix from a Random Forest analysis shows that GBM samples could be separated from control samples, with a 77% predictive accuracy. Thirty of 38 control samples and 29 of 39 pre-radiation samples were correctly classified.

Discussion

Glioblastoma multiforme are a heterogeneous group of tumors based on genomic profiling, yet clinically they have a fairly homogeneous response, with the majority of tumors recurring within 14 m of diagnosis, and within the surgical cavity [19,23]. This homogeneous response suggests common pathways may be found across genetic subgroups. Alternatively, the homogeneous response also suggests that the microenvironment of the tumor, in this case normal brain, may influence the phenotype, and thus, response of the GBM tumor. In this study, we used urinary metabolomic profiling to assess changes in the metabolic processes in patients with GBM. Human urine is a metabolite-rich matrix, readily available *via* non-invasive sampling techniques, and as such, is highly amenable to global metabolic profiling studies in human health and disease [5].

The current study examined urine samples from patients with GBM, compared to those of healthy controls, to look for GBM-specific

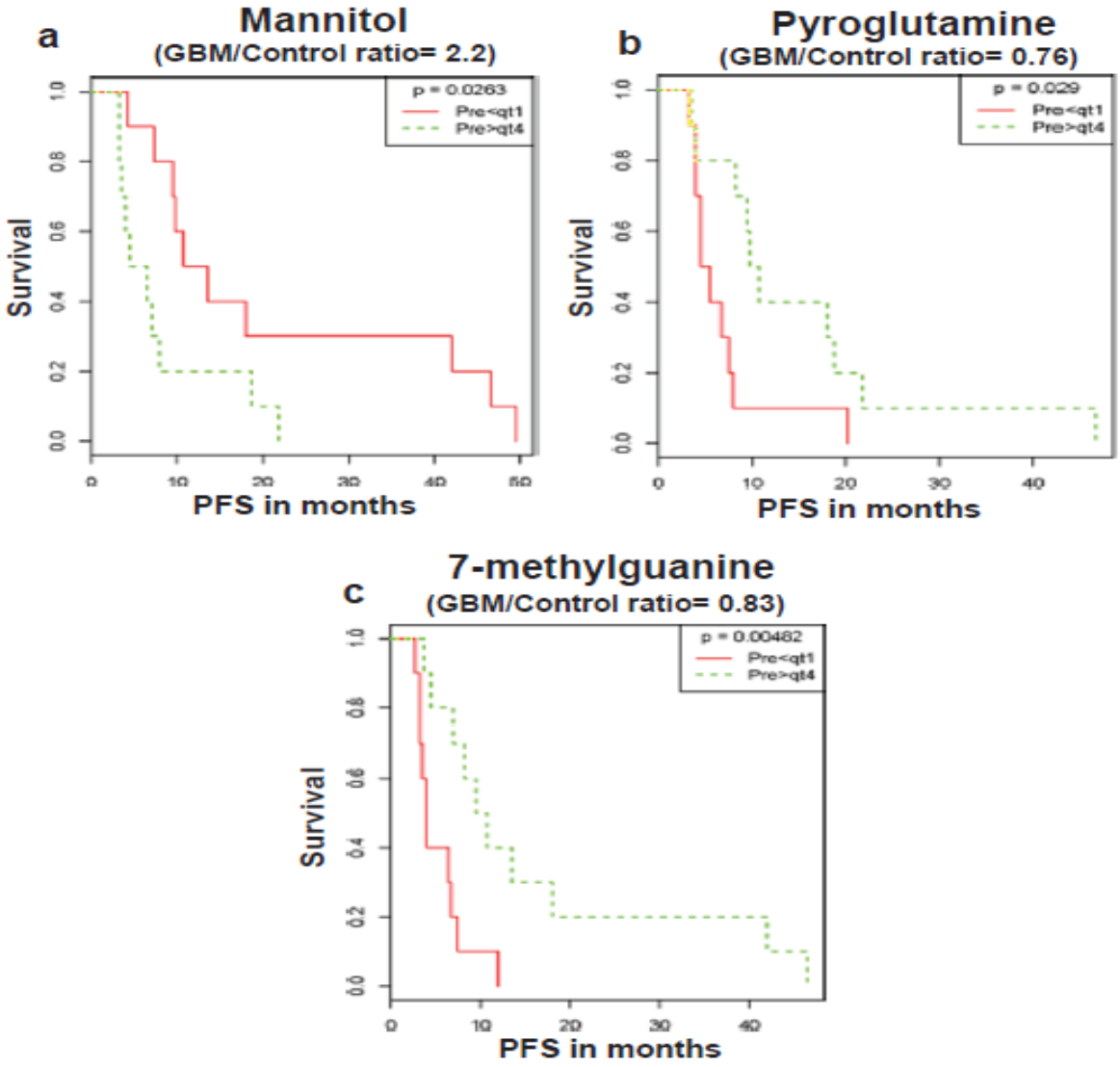

Figure 3: GBM-associated changes in metabolites could affect survival. The significantly different metabolites between GBM and controls were analyzed using a Kaplan-Meier analysis. Three metabolites; mannitol (a), pyroglutamine (b) and 7-methylguanine (c) that were significantly different in pre-radiation (pre-RT) samples (as shown in the ratio), compared to controls, are plotted as a survival curve. Metabolite values across all the pre-RT samples were divided into four quartiles based on the median value. The first quartile (qt1) values were compared to the fourth quartile (qt4) values. The differences were significant, as shown in the respective p values. PFS: progression free survival.

metabolites. Using a combined chromatography/mass spectrometry based approach; we identified 46 significantly altered metabolites in GBM patient urine samples, compared to control samples. Our results suggest significant perturbations in pathways related to amino acid, nucleotide and carbohydrate metabolism. This is consistent with the reported pathways over expressed in samples from patients with GBMs in three recent studies [24-26]. In our study, the specific metabolites, glutamine and N-carbamylglutamate, were both elevated in the urine of patients with GBM. Glutamine is the most abundant amino acid in mammals and acts as fuel for the Krebs cycle. It is also involved in amino acid and protein synthesis, as well as NADPH production, which is required for additional biosynthesis pathways [27]. Wibom et al. [26], showed that glutamate, glutaric acid and pyroglutamic acid were all elevated in GBM samples, compared to "normal" extracellular fluid taken directly from patients, using microdialysis. Likewise, Borodovsky et al. [24] measured increased glutamine in primary tumor samples from patients with gliomas. Extending from these clinical studies, increased glutamine was also measured in tumors, using an orthotopic mouse model of primary human GBM lines; thus, the preclinical model may be recapitulating the clinical scenario, at least for

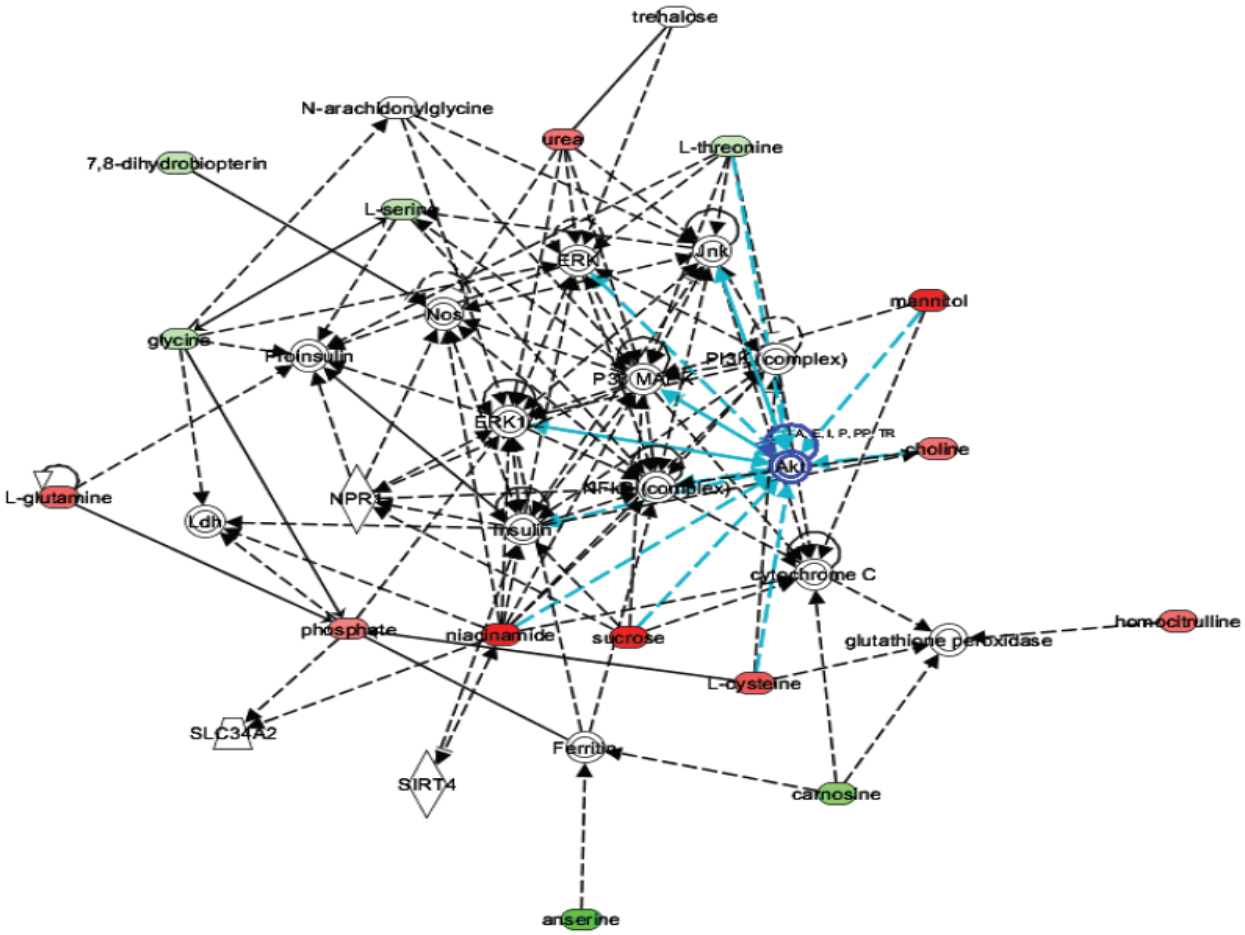

Figure 4: Ingenuity Pathway Analysis of metabolites that differed significantly between GBM groups compared to control (untreated healthy) after a Welch's two-sample *t*-test analysis.

The top network has shown here. This network has the metabolites that were over-expressed in the samples from patients with GBM highlighted in red, and the under expressed metabolites highlighted in green. AKt was identified as a major hub molecule, with direct/indirect interactions with metabolites.

this metabolite [28]. It has been reported that several of the signaling pathways that promote oncogenesis also reprogram glutamine metabolism, leading to tumor cell "glutamine addiction" [29]. To further evaluate the interactions of the metabolites and the underlying signaling pathways that may be involved, we used IPA to run curated comparisons. As shown in figure 4, pathways known to be involved in GBM signaling were found within our networks, including PI3K, AKT and ERK. The PI3K-AKT signal transduction pathway is controlled by the tumor suppressor gene PTEN, which is often deleted or mutated in GBM, leading to the constitutive activation of the PI3K-AKt pathway [30,31]. AKT can also be activated through the mammalian target of rapamycin (mTOR); moreover, Akt activates mTOR among other molecules [32,33]. In our data, we showed an interaction between the AKT pathway and 15 metabolites, significantly altered in GBM. Some of the direct AKT substrates, such as ERK and JNK, are also part of this network. Although from the present study we cannot draw any interpretation of the involvement of AKT, we show how metabolomic approaches may help link the genomic and phenotypic changes seen in GBM [2].

In addition to the GBM only metabolites, we also studied the urine of patients with GBM pre- and post-RT, to identify metabolites that may be produced secondary to radiation exposure. We observed significant alterations in the levels of N-acetylated metabolites and metabolites involved with the TCA cycle following radiation, including citrate, isocitrate, alpha-ketoglutarate, succinate, fumarate and malate. Urinary excretion of acetylated metabolites following radiation has been previously reported [34]. Elevated levels of TCA cycle metabolites were also observed in our study. The excretion of these molecules may be secondary to oxidative stress caused by the radiation. This is consistent with data from Wibom et al. [26], who measured increased citrate and succinate levels in samples from patients with GBM that were irradiated. However, Wibom et al. [26] reported additional molecules from the TCA cycle, not found in our study. These differences may be due to the type of sample used for the metabolomic studies (brain microdialysates in the Wibom et al. [26] and urine in our study), as well as variation of the reference library used in each study. Wibom et al. [26] measured 151 metabolites, but only 67 were "named", compared to the 368 metabolites "named" in our reference library. Recently, studies of low-dose ionizing radiation on mice has shown that metabolites belonging to lipids, amino acids, fatty acids and nucleotides categories were elevated after RT treatment [35,36]. However, further analysis is needed to determine the significance of the elevation of TCA cycle intermediates, after irradiation.

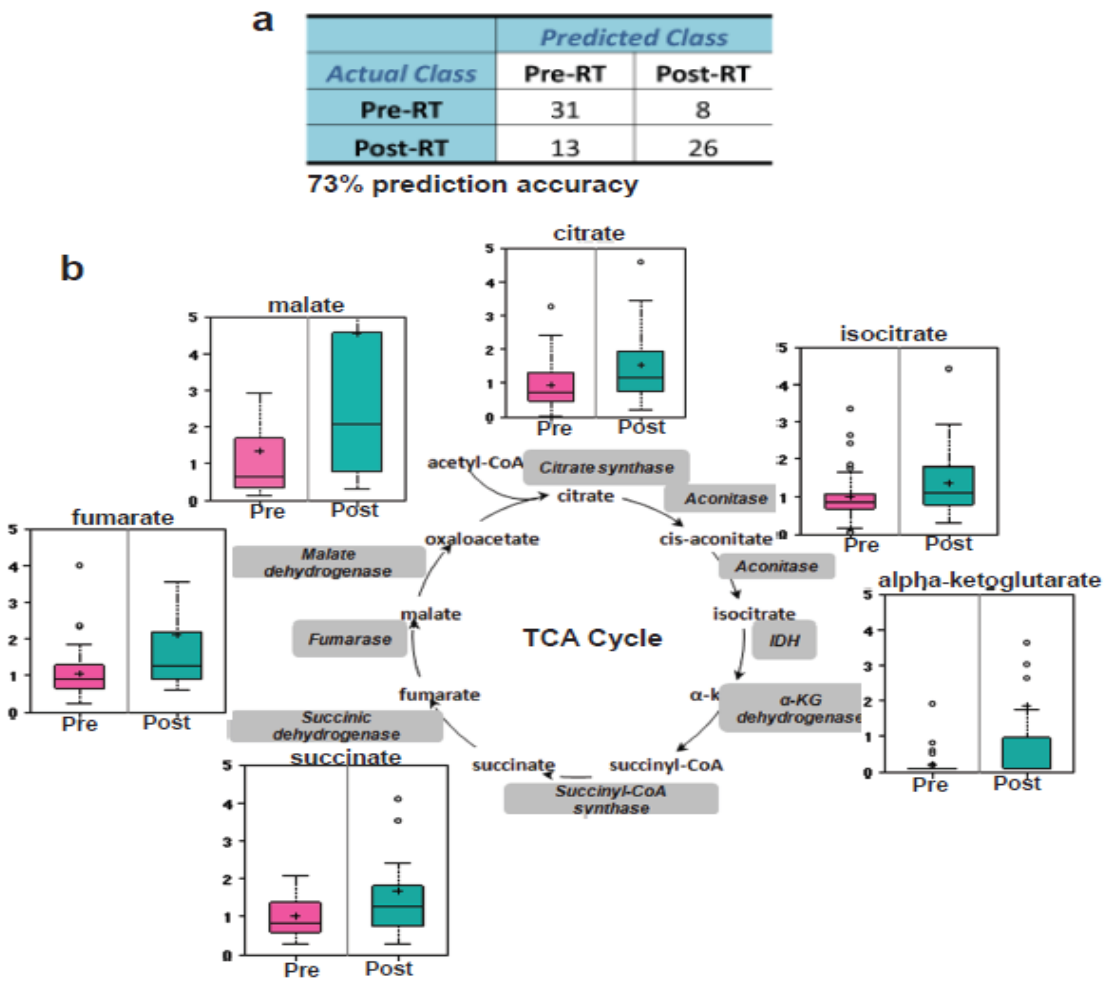

Figure 5: Radiation-induced changes in urine metabolites. Comparison of metabolite levels in pre- and post-radiation (RT) patients using random forest analysis. (a) A predictive accuracy of 73% was obtained for classifying all GBM samples into either pre- or post-RT treatment group. 31 out of 39 pre-RT samples were correctly classified, whereas 26 of the 39 post-RT samples were correctly classified (b) Multiple TCA cycle intermediates accumulated in urine with radiation treatment.

In summary, our study showed a distinct signature of altered urine metabolite levels in GBM patients, with disrupted metabolic pathways related to amino acid, carbohydrate and nucleotide metabolism. The alterations in several metabolites were correlated to progression free survival in the patients with GBM. Additionally, altered metabolites following irradiation were distinct from those found in patients, prior to irradiation, and may be useful as biomarkers of radiation exposure. These results demonstrate the use of metabolomics in the study of GBM disease pathology and biomarker discovery.

Acknowledgements

This research was supported by the Intramural Research Program of the National Institutes of Health, National Cancer Institute. We also acknowledge Dr. David Goldstein in the Office of Science and Technology Partnerships for additional financial support. The assistance of Philip Gunst and Jacob Wulff in the preliminary statistical analysis of the data is gratefully acknowledged.

References

1. Madsen R, Lundstedt T, Trygg J (2010) Chemometrics in metabolomics--a review in human disease diagnosis. Anal Chim Acta 659: 23-33.
2. Vinayavekhin N, Homan EA, Saghatelian A (2010) Exploring disease through metabolomics. ACS Chem Biol 5: 91-103.
3. Hirayama A, Kami K, Sugimoto M, Sugawara M, Toki N, et al. (2009) Quantitative metabolome profiling of colon and stomach cancer microenvironment by capillary electrophoresis time-of-flight mass spectrometry. Cancer Res 69: 4918-4925.
4. Hu JD, Tang HQ, Zhang Q, Fan J, Hong J, et al. (2011) Prediction of gastric cancer metastasis through urinary metabolomic investigation using GC/MS. World J Gastroenterol 17: 727-734.
5. Kim K, Aronov P, Zakharkin SO, Anderson D, Perroud B, et al. (2009) Urine metabolomics analysis for kidney cancer detection and biomarker discovery. Mol Cell Proteomics 8: 558-570.
6. Kind T, Tolstikov V, Fiehn O, Weiss RH (2007) A comprehensive urinary metabolomic approach for identifying kidney cancerr. Anal Biochem 363: 185-195.
7. Mal M, Koh PK, Cheah PY, Chan EC (2009) Development and validation of a gas chromatography/mass spectrometry method for the metabolic profiling of human colon tissue. Rapid Commun Mass Spectrom 23: 487-494.
8. Monleón D, Morales JM, Barrasa A, López JA, Vázquez C, et al. (2009) Metabolite profiling of fecal water extracts from human colorectal cancer. NMR Biomed 22: 342-348.

9. Qiu Y, Cai G, Su M, Chen T, Liu Y, et al. (2010) Urinary metabonomic study on colorectal cancer. J Proteome Res 9: 1627-1634.

10. Qiu Y, Cai G, Su M, Chen T, Zheng X, et al. (2009) Serum metabolite profiling of human colorectal cancer using GC-TOFMS and UPLC-QTOFMS. J Proteome Res 8: 4844-4850.

11. Tan C, Chen H, Xia C (2009) Early prediction of lung cancer based on the combination of trace element analysis in urine and an Adaboost algorithm. J Pharm Biomed Anal 49: 746-752.

12. Wu H, Xue R, Lu C, Deng C, Liu T, et al. (2009) Metabolomic study for diagnostic model of oesophageal cancer using gas chromatography/mass spectrometry. J Chromatogr B Analyt Technol Biomed Life Sci 877: 3111-3117.

13. Jonsson P, Johansson AI, Gullberg J, Trygg J, A J, et al. (2005) High-throughput data analysis for detecting and identifying differences between samples in GC/MS-based metabolomic analyses. Anal Chem 77: 5635-5642.

14. Jonsson P, Gullberg J, Nordström A, Kusano M, Kowalczyk M, et al. (2004) A strategy for identifying differences in large series of metabolomic samples analyzed by GC/MS. Anal Chem 76: 1738-1745.

15. Kirk MJ, Hayward RM, Sproull M, Scott T, Smith S, et al. (2008) Non-patient related variables affecting levels of vascular endothelial growth factor in urine biospecimens. J Cell Mol Med 12: 1250-1255.

16. Evans AM, DeHaven CD, Barrett T, Mitchell M, Milgram E (2009) Integrated, nontargeted ultrahigh performance liquid chromatography/electrospray ionization tandem mass spectrometry platform for the identification and relative quantification of the small-molecule complement of biological systems. Anal Chem 81: 6656-6667.

17. Dehaven CD, Evans AM, Dai H, Lawton KA (2010) Organization of GC/MS and LC/MS metabolomics data into chemical libraries. J Cheminform 2: 9.

18. Storey JD, Tibshirani R (2003) Statistical significance for genomewide studies. Proc Natl Acad Sci U S A 100: 9440-9445.

19. Masica DL, Karchin R (2011) Correlation of somatic mutation and expression identifies genes important in human glioblastoma progression and survival. Cancer Res 71: 4550-4561.

20. McDowell KA, Riggins GJ, Gallia GL (2011) Targeting the AKT pathway in glioblastoma. Curr Pharm Des 17: 2411-2420.

21. Rekers NH, Sminia P, Peters GJ (2011) Towards tailored therapy of glioblastoma multiforme. J Chemother 23: 187-199.

22. Brennan C (2011) Genomic profiles of glioma. Curr Neurol Neurosci Rep 11: 291-297.

23. Hegi ME, Diserens AC, Gorlia T, Hamou MF, de Tribolet N, et al. (2005) MGMT gene silencing and benefit from temozolomide in glioblastoma. N Engl J Med 352: 997-1003.

24. Borodovsky A, Seltzer MJ, Riggins GJ (2012) Altered cancer cell metabolism in gliomas with mutant IDH1 or IDH2. Curr Opin Oncol 24: 83-89.

25. Chinnaiyan P, Kensicki E, Bloom G, Prabhu A, Sarcar B, et al. (2012) The metabolomic signature of malignant glioma reflects accelerated anabolic metabolism. Cancer Res 72: 5878-5888.

26. Wibom C, Surowiec I, Mörén L, Bergström P, Johansson M, et al. (2010) Metabolomic patterns in glioblastoma and changes during radiotherapy: a clinical microdialysis study. J Proteome Res 9: 2909-2919.

27. Dell' Antone P (2012) Energy metabolism in cancer cells: how to explain the Warburg and Crabtree effects? Med Hypotheses 79: 388-392.

28. Marin-Valencia I, Yang C, Mashimo T, Cho S, Baek H, et al. (2012) Analysis of tumor metabolism reveals mitochondrial glucose oxidation in genetically diverse human glioblastomas in the mouse brain *in vivo*. Cell Metab 15: 827-837.

29. Wise DR, Thompson CB (2010) Glutamine addiction: a new therapeutic target in cancer. Trends Biochem Sci 35: 427-433.

30. Endersby R, Baker SJ (2008) PTEN signaling in brain: neuropathology and tumorigenesis. Oncogene 27: 5416-5430.

31. Houillier C, Lejeune J, Benouaich-Amiel A, Laigle-Donadey F, Criniere E, et al. (2006) Prognostic impact of molecular markers in a series of 220 primary glioblastomas. Cancer 106: 2218-2223.

32. Zoncu R, Efeyan A, Sabatini DM (2011) mTOR: from growth signal integration to cancer, diabetes and ageing. Nat Rev Mol Cell Biol 12: 21-35.

33. Hahn-Windgassen A, Nogueira V, Chen CC, Skeen JE, Sonenberg N, et al. (2005) Akt activates the mammalian target of rapamycin by regulating cellular ATP level and AMPK activity. J Biol Chem 280: 32081-32089.

34. Johnson CH, Patterson AD, Krausz KW, Lanz C, Kang DW, et al. (2011) Radiation metabolomics. 4. UPLC-ESI-QTOFMS-Based metabolomics for urinary biomarker discovery in gamma-irradiated rats. Radiat Res 175: 473-484.

35. Tyburski JB, Patterson AD, Krausz KW, Slavík J, Fornace AJ Jr, et al. (2009) Radiation metabolomics. 2. Dose- and time-dependent urinary excretion of deaminated purines and pyrimidines after sublethal gamma-radiation exposure in mice. Radiat Res 172: 42-57.

36. Lee do Y, Bowen BP, Nguyen DH, Parsa S, Huang Y, et al. (2012) Low-dose ionizing radiation-induced blood plasma metabolic response in a diverse genetic mouse population. Radiat Res 178: 551-555.